INTERNATIONAL JOURNAL OF SCIENTIFIC RESEARCH AND INNOVATIVE STUDIES

IJSRIS journal

ISSN: 2820-7157

Advancing Knowledge, Inspiring Innovation

www.ijsrisjournal.com

INDEXED JOURNAL

PEER REVIEWED Rigorous & Transparent | DOI: CROSSREF Member | OPEN ACCESS For Global Visibility | BI-MONTHLY Timely Publication | WIDE READERSHIP High Impact & Visibility | AUTHOR FRIENDLY Fast | Supportive | Reliable

RECEIVED 19 June 2026 | ACCEPTED 10 July 2026 | PUBLISHED 1 August 2026

August 2026 | Volume 5 | Number 4

Pages from: 1101 to 1110

NAmbOA: A Hybrid Metaheuristic for Energy-Prioritized Multi-Objective Route Optimization in RPL-Based 6LoWPAN IoT Networks

KONE Kigninman Désiré[1], GBEGBE Raymond[2], DJE Bi Irié Cyrille[1], ASSEU Pascal Olivier[1,2]

[1]LASTIC, Ecole Supérieure Africaine des TIC (ESATIC), Abidjan, Côte d'Ivoire, desire.kone@esatic.edu.ci
[2]UMRI-STI, Institut National Polytechnique Félix Houphouët-Boigny (INP-HB), Yamoussoukro, Côte d'Ivoire

LICENSE

This article is licensed under the Creative Commons Attribution 4.0 International License (CC BY 4.0).

https://creativecommons.org/licenses/by/4.0/

Crossref doi

PREFIX : 10.63883

IJSRIS JOURNAL

OPEN ACCESS

This is an open access article distributed under the terms of open access.

ABSTRACT

Energy consumption remains a major concern in RPL-based 6LoWPAN networks, where constrained devices operate with limited battery, processing, and communication resources. This paper presents an energy-prioritized six-objective routing framework that jointly considers Average Energy Consumption (AEC), Convergence Time (CT), Packet Overhead (PoH), Packet Delivery Ratio (PDR), Average Path Length (APL), and End-to-End Delay (EED) over DODAG-compatible routes. For the primary source-level experiment, every route in the complete candidate set ($K \leq 5$) is evaluated and the minimum-fitness route is selected exactly; no metaheuristic advantage is claimed for this small discrete problem. The NAmbOA hybrid search, combining NiOA-inspired diversification and CAOA-inspired leader-guided intensification, is evaluated separately in a coupled network-wide parent-selection problem. On 200-node controlled instances, the energy-priority formulation reduces mean AEC by 23.35% relative to an ETX-minimizing/MRHOF-like reference, with modest differences in the reported overhead, delay, and delivery endpoints. Across 30 paired network-wide instances, NAmbOA obtains lower final fitness than the NiOA-inspired and CAOA-inspired component-only variants, while no significant convergence-speed advantage is observed. The results support an energy-centered routing trade-off and a network-wide hybrid-search contribution under the stated simulator assumptions; they do not constitute validation of a full standards-compliant RPL implementation.

Keywords: Energy efficiency; routing reliability; packet delivery; path selection; convergence behavior; objective function.

1. Introduction

IPv6 over Low-Power Wireless Personal Area Networks (6LoWPAN) enables IPv6 connectivity for resource-constrained Internet of Things (IoT) devices. In these networks, the IPv6 Routing Protocol for Low-Power and Lossy Networks (RPL) organizes nodes into a Destination-Oriented Directed Acyclic Graph (DODAG) rooted at a sink or border router [1]. Although RPL is designed for constrained environments, route selection remains challenging because wireless links are lossy and nodes have limited energy, memory, processing, and communication resources.

Energy consumption is particularly important because transmission, reception, control signaling, and multi-hop forwarding directly affect network lifetime. However, minimizing energy alone may lead to undesirable routing behavior, including increased delay, reduced delivery reliability, higher routing overhead, slower convergence, or inefficient paths. Energy-aware routing should therefore account for these competing requirements rather than optimize energy in isolation.

Recent studies have explored energy-aware and multi-metric RPL routing through optimization, queue- and workload-aware mechanisms, Tabu Search, and fuzzy objective functions [2] – [6]. Trust-based routing and intrusion-detection studies [7] – [9] are relevant to the broader reliability context, but their primary objective is security rather than energy-prioritized route optimization. A remaining methodological question is how much of an observed benefit comes from the objective weights and how much comes from the search mechanism itself.

To address this question, the study separates two levels of analysis. At source level, six normalized routing objectives are aggregated with explicit energy priority and the best route is selected by complete enumeration of the small DODAG-compatible candidate set. At network level, the coupled parent-selection problem is searched with NAmbOA, which combines NiOA-inspired diversification with CAOA-inspired leader-guided intensification.

The primary research question is whether explicit energy prioritization reduces AEC without disproportionate degradation in the reported routing endpoints. The secondary question is whether the NiOA–CAOA hybrid improves final fitness relative to its component-only variants in the larger coupled network-wide formulation.

The main contributions of this study are:

- An explicit, reproducible six-objective formulation over DODAG-compatible routes, with energy prioritized and the complete source-level candidate set evaluated exactly.
- A network-wide NAmbOA search that combines NiOA-inspired diversification with CAOA-inspired leader-guided intensification, assessed separately from the weighting effect.
- Paired controlled experiments, weighting and component ablations, and network-size/density sensitivity analyses that delimit the claims supported by the available results.

The remainder of the paper is organized as follows. Section 2 presents the background, related work, and research gap. Section 3 describes the system model, multi-objective routing formulation, proposed NAmbOA search mechanism, and experimental methodology. Section 4 presents the experimental results and ablation analyses. Section 5 discusses the main findings and limitations. Section 6 concludes the paper and outlines directions for future work.

2. Background

In RPL-based 6LoWPAN networks, energy-efficient routing must balance several potentially conflicting requirements. Reducing energy consumption may come at the cost of reliability, latency, routing overhead, convergence speed, or path efficiency. Existing approaches therefore differ in the metrics they consider and, in the mechanisms, used to manage these trade-offs.

2.1. Literature Review

Several recent studies have investigated energy-aware and multi-metric routing in RPL-based IoT networks. Mokrani et al. [2] proposed LEA-RPL, which uses particle swarm optimization to combine expected lifetime, delay, and energy-aware ETX in parent selection. Diniesh et al. [3] introduced MQW-RPL, incorporating ETX, energy, RSSI, queue conditions, workload, and mobility information to improve energy efficiency and load distribution. Tarif et al. [4] used Tabu Search to optimize RPL routing according to residual energy, transmission energy, distance, hop count, ETX, and link stability. Other approaches include the fuzzy cross-layer objective function proposed by Poornima et al. [5] and the optimization-based routing mechanisms studied by Lmkaiti et al. [6], which consider ETX, latency, and energy.

Among these approaches, LEA-RPL is particularly relevant because it combines energy-related and routing-performance criteria and evaluates energy consumption, convergence time, control overhead, end-to-end delay, and packet delivery ratio in Contiki/Cooja [2]. However, direct numerical comparison is not appropriate because the simulation models and experimental conditions differ.

NiOA [10] and CAOA [11] are recent metaheuristics that use complementary exploration and exploitation mechanisms. NiOA provides diversification-oriented search operations, whereas CAOA employs leader-guided mechanisms that support intensification.

2.2. Research Gap

Existing studies show that energy can be combined with other routing metrics in RPL networks. However, explicit energy prioritization is often confounded with the optimizer used to implement it. This study addresses that gap by evaluating the objective formulation through exact source-level route comparison and evaluating hybrid search only in a larger network-wide decision space. The distinction is essential because applying a population metaheuristic to no more than five fully evaluated candidates would add complexity without changing the exact optimum.

3. Material and Methods

3.1. System Model and DODAG Construction

The considered RPL-based 6LoWPAN network is represented by a graph $G = (V, E)$, where $V = \{v_0, v_1, \ldots, v_{n-1}\}$ is the set of nodes and E is the set of wireless links. Node v_0 represents the sink/root, while the remaining nodes may act as traffic sources or forwarding nodes. Each wireless link is characterized by link-quality, energy, delay, and packet-loss attributes.

RPL organizes the network as a Destination-Oriented Directed Acyclic Graph (DODAG) rooted at v_0. In the considered model, the DODAG is initialized using ETX-weighted shortest-path distances to the root. These distances define the rank associated with each node and determine the feasible routing space subsequently explored by exact source-level enumeration.

For each non-root node v_i, the admissible parent set is defined as $A(v_i) = \{v_j \in N(v_i) \mid \mathrm{Rank}(v_j) < \mathrm{Rank}(v_i)\}$, where $N(v_i)$ denotes the set of neighbors of v_i. A forwarding transition is allowed only toward a strictly lower-rank neighbor. This strict rank decrease ensures monotonic progress toward the root and makes cyclic forwarding paths infeasible within the candidate-routing space.

For a source node s, a feasible route is represented as $P_s = (s, v_{i1}, v_{i2}, \ldots, v_0)$, subject to $\mathrm{Rank}(v_{ik+1}) < \mathrm{Rank}(v_{ik})$ for every forwarding transition. Candidate routes are therefore constructed within the DODAG rather than from arbitrary loop-free paths of the underlying physical graph.

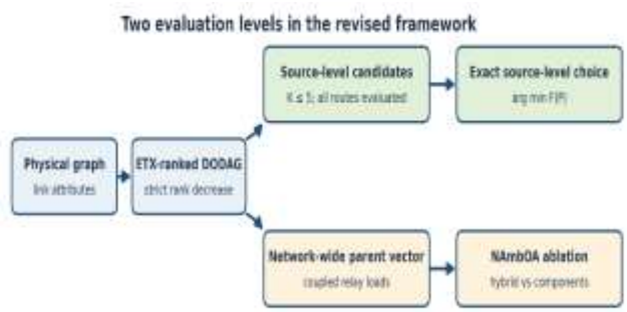

Fig. 1. Separation of exact source-level route selection from network-wide NAmbOA hybridization analysis.

3.2. DODAG-Constrained Candidate Route Generation

For each selected non-root source s, a finite set of DODAG-compatible candidate routes is constructed as $P_s^{DODAG} = \{P_{s,1}, P_{s,2}, \ldots, P_{s,K}\}$ where (K) denotes the maximum number of candidate routes retained for source s. Candidate generation is performed only over the directed rank-decreasing graph defined in Section 3.1. Several routing criteria are used to obtain alternative feasible paths, including ETX, energy cost, delay, packet loss, hop count, and composite link costs.

Regardless of the criterion used to generate a candidate route, each forwarding transition must satisfy the strict rank constraint. Consequently, every candidate route must terminate at the root and contain only transitions toward lower-rank neighbors. In the primary experiments, a maximum of five candidate routes is retained for each selected source $K = 5$.

The RPL/DODAG constraints define the feasible source-level routing space. Because at most five unique routes are retained and their fitness values are fully available, the primary experiment evaluates all candidates and selects the exact minimum. NAmbOA is reserved for the coupled network-wide formulation described in Section 3.5.2.

3.3. Multi-Objective Route Formulation

Each DODAG-compatible candidate path is evaluated using six routing objectives: Average Energy Consumption (AEC), Convergence Time (CT), Packet Overhead (PoH), Packet Delivery Ratio (PDR), Average Path Length (APL), and End-to-End Delay (EED). The adopted formulations are consistent with those reported for AEC, CT, and PoH in [2], and for PDR, APL, and EED in [4]. These metrics are also widely used to evaluate routing performance in RPL-based networks [3].

For each candidate path P, the corresponding metric values are computed using the controlled estimators specified in Section 3.6. AEC, CT, PoH, APL, and EED are minimized, whereas PDR is maximized. The same equations are applied to every compared route-selection method.

Before aggregation, the six objectives are normalized to prevent differences in scale from dominating the optimization process. Energy consumption is given the highest priority in the primary configuration, while the remaining metrics are retained to control undesirable routing trade-offs. The resulting objective function is then used by exact enumeration to evaluate and select routes from the DODAG-compatible candidate set.

3.4. Normalization and Energy-Prioritized Fitness Function

For each source-specific candidate set, a minimized metric m is normalized as $\hat{m}(P) = [m(P) - m_{min}]/[m_{max} - m_{min} + \varepsilon]$, with $\varepsilon > 0$ preventing division by zero. PDR is converted to a cost as $1 - \widehat{PDR}(P)$, where $\widehat{PDR}$ uses the same min–max denominator. All hatted quantities in the fitness function therefore lie in [0,1] up to ε.

The energy-prioritized fitness function is defined as:

$$F(P) = 0.40\,\widehat{AEC}(P) + 0.12\,\widehat{CT}(P) + 0.12\,\widehat{PoH}(P) + 0.12[1 - \widehat{PDR}(P)] + 0.12\,\widehat{APL}(P) + 0.12\,\widehat{EED}(P).$$

Energy receives the largest weight 0.40, while each of the remaining objectives is assigned a weight of 0.12. This configuration prioritizes energy reduction while retaining the other routing metrics to limit adverse performance trade-offs. The 0.40 energy weight represents the primary configuration evaluated in this study rather than a universally optimal weighting, and its influence is examined through the weighting ablation reported in the experimental section.

For each source s, the selected route is $P_s^* = \arg\min\{F(P): P \in P_s^{DODAG}\}$. Since $K \leq 5$, this arg min is obtained by exhaustive comparison in the primary source-level experiments.

3.5. NAmbOA Search Mechanism and Scope

NAmbOA combines mechanisms inspired by the Ninja Optimization Algorithm (NiOA) [10] and the Crocodile Ambush Optimization Algorithm (CAOA) [11]. NiOA-inspired peer-based moves and stochastic perturbation promote diversification, whereas CAOA-inspired leader guidance promotes intensification. The hybrid is treated as a network-wide search heuristic; it is not needed to solve the fully enumerated $K \leq 5$ source-level problem.

For a discrete candidate index, a continuous position x is decoded as $k = \mathrm{clip}(\mathrm{round}(x), 1, K)$. For the network-wide problem, an agent encodes one admissible lower-rank parent for every non-root node, $X = (p_1, \ldots, p_{n-1})$. After every continuous update, each coordinate is bounded and decoded to an admissible parent index before evaluation.

Diversification, stochastic perturbation, and leader-guided intensification are applied in that order. The decoded network is evaluated only after admissibility repair, so every retained parent points to a strictly lower-rank neighbor.

A proposed decoded solution replaces the current solution when its fitness is no worse. A stochastic perturbation is applied with probability $p_m = 0.3$. If the global best does not improve for $S_t = 3$ iterations, the worst quarter of the population is reinitialized. The experiments use $N = 80$ and $T_{max} = 200$.

3.5.1. Overall NAmbOA Routing Procedure

Algorithm 1 separates exact source-level selection from the network-wide heuristic study. This prevents improvements due to the energy-prioritized objective from being attributed automatically to the metaheuristic.

Algorithm 1. DODAG-Constrained Energy-Prioritized Route Selection and Network-Wide NAmbOA Study

Input: G= (V, E), root v_0, sources S, K≤5, weights w, N=80, T_{max}=200, p_m=0.3, S_t=3.

Output: exact source-level routes and network-wide ablation solutions.

Phase I — DODAG and candidates

1: Compute ETX-based ranks and admissible lower-rank parent sets $A(v_i)$.

2: Generate up to K unique loop-free DODAG-compatible routes per source.

Phase II — exact source-level evaluation

3: Compute the six metrics, normalize them within each source candidate set, and evaluate F(P).

4: Select $P_s^* = \arg\min\{F(P): P \in P_s^{DODAG}\}$ by exhaustive comparison.

Phase III — network-wide NAmbOA ablation

5: Encode an agent as $X=(p_1,\ldots,p_{n-1})$, one admissible parent per non-root node.

6: Initialize N agents; decode/repair each coordinate and identify the global best.

7: For $t=1,\ldots,T_{max}$, apply NiOA-inspired peer diversification and perturb with probability p_m.

8: Apply CAOA-inspired leader guidance; bound, decode, repair, and evaluate the network.

9: Accept a non-worse decoded solution and update the global best.

10: After S_t stagnant iterations, reinitialize the worst N/4 agents.

11: Return the final global best for full NAmbOA and repeat under identical budgets for each component-only variant.

3.5.2. Network-Wide Formulation for Hybridization Analysis

For each non-root node v_i, the decision variable p_i selects one parent from $A(v_i)$, yielding $X = (p_1, \ldots, p_{n-1})$. The decoded parent vector induces a complete rank-decreasing forwarding structure. Unlike independent source-level choices, node decisions are coupled because relay load depends on how many source-to-root paths traverse each node and link; this coupling affects the aggregated energy, delivery, overhead, path-length, convergence, and delay estimators. For each minimized network metric m, the ablation uses the bounded cost $n_m(X) = m(X)/[m(X) + mref]$, where mref is the value of a deterministic ETX-RPL reference on the same instance; delivery is represented as $1 - PDR(X)/100$. The six costs are combined using the energy-priority weights. The same 30 paired instances, initialization protocol, evaluation budget, and decoding rule are used for full NAmbOA and both component-only variants.

3.6. Routing Metrics and Simulation Model

The six-routing metrics are computed from the same link attributes and equations for all methods. For a route P with H links, $ETX(P) = \Sigma_e \in P\ ETX_e$, $E(P) = \Sigma_e \in P\ E_e$, $D(P) = \Sigma_e \in P\ D_e$, and APL(P) = H.

The controlled simulator uses a static 100 × 100 m deployment, nominal range 40 m, packet length L = 80 bytes, and data rate R = 250 kbps. For a link of length d, $b = 1 + (d/40)^2$; $ETX_e = b + |N(0,0.15)|$; E_e and D_e are sampled independently as $bU(0.6,1.8) + |N(0,0.4)|$; and loss ℓ_e is $clip[0.01 + 0.14(d/40)^2 + |N(0,0.02)|, 0.005, 0.35]$. These stochastic terms are resampled with the topology seed and are shared by all paired methods.

If a random deployment contains disconnected components, the nearest pair of nodes in distinct components is connected iteratively before DODAG construction. These repair links are synthetic connectivity devices and are evaluated by the same distance-dependent link model; they are not claimed to reproduce a physical deployment intervention.

The path estimators are $AEC(P) = 120(e_{tx} + e_{rx} + eCPU + eidle)E(P)$, with $(e_{tx},e_{rx},eCPU,eidle) = (0.5,0.3,0.1,0.05)$; $CT(P) = 20H + 5ETX(P)$; $PoH(P) = 100[2H + ETX(P)]/[100 + 2H + ETX(P)]$; $PDR(P) = 100\prod_e \in P(1 - \ell_e)$; and $EED(P) = H(1000L/R + 2) + 6D(P)$, with L expressed in bits. AEC is a model-calibrated millijoule-scale estimator, not a hardware measurement. The simulator operates at routing/path level and does not reproduce the complete IEEE 802.15.4, 6LoWPAN, or RPL control stack.

3.7. Experimental Setup and Reference Methods

Experiments are conducted on independently generated RPL-based 6LoWPAN network instances. The main simulation parameters are summarized in Table 1. Since the deployment area is fixed while the number of nodes increases, the corresponding experiment is interpreted as a joint network-size and density sensitivity analysis rather than as a pure scalability study.

For the primary source-level experiments, 25 non-root nodes are sampled per 200-node instance (or all available non-root nodes if fewer) as traffic sources. For each source, up to five unique loop-free DODAG-compatible routes are generated using ETX, energy, delay, loss, hop-count, and randomly weighted composite link criteria. Every retained route is evaluated and the exact minimum-fitness route is selected.

The primary reference method is an ETX-minimizing/MRHOF-like strategy [12], which selects the DODAG-compatible route with the lowest accumulated ETX. The term MRHOF-like is used because the simulator reproduces the ETX-minimization principle relevant to the comparison without implementing the complete MRHOF control process.

The second reference method is an energy-greedy strategy that selects the candidate route with the minimum AEC. This baseline represents pure energy minimization and is used to assess the trade-offs associated with optimizing energy alone.

Paired experiments use the same topology, link attributes, candidate routes, and source set across compared methods. The network-wide hybridization ablation uses 30 paired 200-node instances and the common population and iteration settings stated in Section 3.5.

Table 1. Main experimental settings.

Parameter	**Value**
Deployment area	100 × 100 m
Network size	50, 100, 150, and 200 nodes
Sink/root	Near one corner of the deployment area
Nominal transmission range	40 m
Data rate	250 kbps
Packet size	80 bytes
Candidate routes per source	Up to K = 5 DODAG-compatible paths
Primary weight vector	(0.40, 0.12, 0.12, 0.12, 0.12, 0.12)
Primary comparison runs	10 paired independent runs
Weighting-ablation runs	12 independent runs
Network-wide hybridization runs	30 paired independent runs
Statistical test	Paired Wilcoxon signed-rank test, $\alpha = 0.05$
Source nodes per 200-node source-level run	25 randomly sampled non-root nodes
Source-level decision rule	Exact argmin over all retained $K \leq 5$ candidates
NAmbOA search settings	$N = 80$; $T_{max} = 200$; $p_m = 0.3$; $S_t = 3$
Connectivity repair	Nearest disconnected components linked before DODAG construction

3.8. Statistical Analysis

Results are reported as mean ± standard deviation across independently generated network instances; each instance, rather than each source route, is the experimental unit. Source-level metrics are first aggregated within an instance, preventing pseudo replication.

Paired comparisons use the two-sided Wilcoxon signed-rank test because the same network instances are evaluated by each method and normality of paired differences is not assumed. The significance threshold is 0.05. For the four network-size AEC tests, Holm correction controls family-wise error; other reported p-values belong to separately prespecified comparisons and are interpreted with their observed effect magnitudes.

The analysis distinguishes the primary routing comparison, weighting ablation, network-size/density sensitivity, and network-wide hybridization ablation. No inference treats multiple sources from one topology as independent replicates.

4. Results

4.1. Overall Routing Performance

The primary comparison tests the energy-priority objective against an ETX-minimizing/MRHOF-like route reference and the energy-only extreme. Table 2 reports the four endpoints retained in the run-level result summaries. CT and APL enter route fitness but are not reported as outcome tables; conclusions are therefore restricted to AEC, PoH, EED, and PDR.

Table 2. Routing performance for 200-node networks (mean ± SD over 10 paired runs).

Method	AEC (mJ)	PoH (%)	EED (ms)	PDR (%)
Energy-priority (exact)	445.79 ± 33.85	7.81 ± 0.57	41.26 ± 2.91	76.64 ± 1.56
ETX-minimizing/MRHOF-like	581.61 ± 50.88	7.56 ± 0.56	40.84 ± 3.30	77.11 ± 1.84
Energy-greedy	398.37 ± 20.21	8.61 ± 0.73	46.97 ± 4.07	76.29 ± 1.57

The exact source-level selector reduces mean AEC by 23.35% compared with the ETX-minimizing/MRHOF-like reference. Mean PoH, EED, and PDR differ by 0.25 percentage points, 0.42 ms, and −0.47 percentage points, respectively. The energy-greedy baseline attains still lower AEC but increases PoH and EED, illustrating the trade-off rather than universal dominance of the proposed weighting.

4.2. Effect of Energy Prioritization

To isolate objective weighting, four configurations were evaluated over 12 independent 200-node instances with identical candidate sets and exact source-level selection: energy-priority (0.40,0.12,0.12,0.12,0.12,0.12), balanced (1/6 for every metric), overhead-priority (0.12,0.12,0.40,0.12,0.12,0.12), and reliability-priority (0.12,0.12,0.12,0.40,0.12,0.12), ordered as (AEC, CT, PoH, PDR cost, APL, EED).

Table 3. Effect of objective weighting at 200 nodes (mean ± SD over 12 runs).

Configuration	AEC (mJ)	PoH (%)	EED (ms)	PDR (%)
Energy-priority	473.29 ± 44.99	7.88 ± 0.65	41.04 ± 4.45	76.49 ± 2.22
Balanced	534.32 ± 59.53	7.78 ± 0.66	39.46 ± 4.06	76.77 ± 2.19
Overhead-priority	551.74 ± 66.18	7.76 ± 0.65	39.98 ± 4.13	76.79 ± 2.23
Reliability-priority	551.36 ± 60.97	7.94 ± 0.65	40.51 ± 4.36	77.53 ± 2.18

Energy-priority weighting reduces mean AEC by 11.42% relative to balanced weighting (paired Wilcoxon $p = 0.000488$). Reliability-priority weighting yields the highest mean PDR, whereas overhead-priority weighting yields the lowest mean PoH. Because the table reports four of the six optimized metrics, the ablation supports controllability of the reported trade-off but not superiority across every objective.

4.3. Network-Size and Density Sensitivity

The robustness of the energy reduction was evaluated across 50, 100, 150, and 200-node configurations. Table 4 compares the AEC obtained with the energy-priority exact source-level selection and the ETX-minimizing/MRHOF-like reference over 10 paired runs per configuration.

Table 4. AEC sensitivity to network size and density (10 paired runs per configuration).

Nodes	Energy-priority (exact) AEC (mJ)	MRHOF-like AEC (mJ)	AEC reduction	Holm-adjusted p-value
50	508.27	598.96	15.14%	0.007812
100	481.67	590.26	18.40%	0.007812
150	469.11	580.21	19.15%	0.007812
200	445.79	581.61	23.35%	0.007812

The energy-priority selector has lower mean AEC than the ETX-minimizing/MRHOF-like reference at every evaluated size/density. The reduction ranges from 15.14% to 23.35%. Each raw paired Wilcoxon p-value is 0.001953; after Holm correction across the four size comparisons, the adjusted p-value is 0.007812 for each comparison.

Because network size and density increase simultaneously in the fixed deployment area, the observed trend should be interpreted as a joint size-and-density effect rather than as evidence of pure scalability.

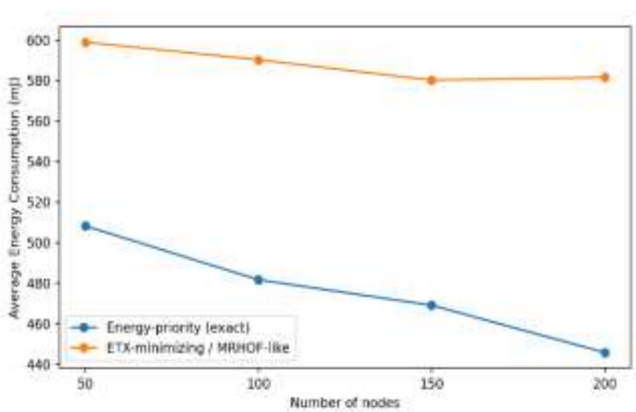

Fig. 2. AEC versus network size for energy-priority exact source-level selection and the ETX-minimizing/MRHOF-like baseline over 10 paired runs per configuration.

4.4. Hybridization Ablation

The contribution of hybrid search is evaluated only in the coupled network-wide formulation. In the source-level problem, all $K \leq 5$ candidate fitness values are known and exact enumeration is both simpler and guaranteed to identify the minimum; a population search would be methodologically unnecessary.

The network-wide formulation couples one lower-rank parent choice per non-root node through relay loads and evaluates full NAmbOA against NiOA-inspired and CAOA-inspired component-only variants under a common budget. This experiment tests hybridization, whereas Tables 2–4 primarily test the energy-prioritized formulation.

Table 5. Network-wide hybridization ablation over 30 paired independent 200-node instances (mean ± SD).

Algorithm	Final fitness	Convergence iteration
NAmbOA	0.6784 ± 0.0331	39.23 ± 10.50
NiOA-inspired component only	0.7017 ± 0.0326	38.63 ± 10.02
CAOA-inspired component only	0.7514 ± 0.0269	36.80 ± 8.64

NAmbOA achieves mean final fitness 0.6784, compared with 0.7017 for the NiOA-inspired component-only variant and 0.7514 for the CAOA-inspired component-only variant. The paired differences favor NAmbOA versus CAOA-inspired ($p < 0.000001$) and NiOA-inspired ($p = 0.000003$) under the evaluated 30-instance protocol.

For convergence speed, NAmbOA does not achieve the lowest mean convergence iteration. However, the paired differences are not statistically significant relative to either the NiOA-inspired variant ($p=0.810956$) or the CAOA-inspired variant ($p=0.190255$).

The ablation supports improved final solution quality under this specific coupled formulation and budget; it does not establish general superiority across other network models, parameter settings, or metaheuristics.

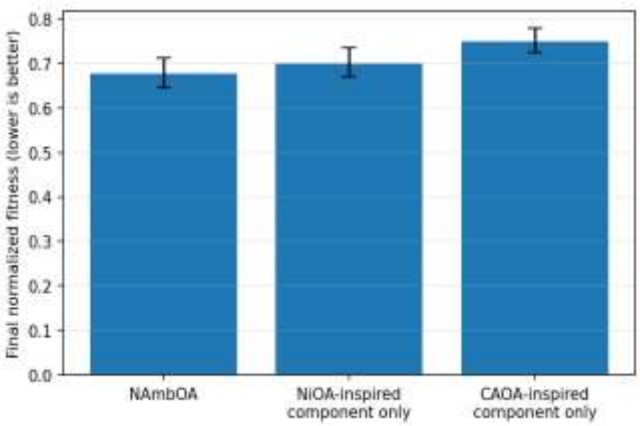

Fig. 3. Network-wide final fitness for NAmbOA and the two component-only variants over 30 independent instances (mean ± SD).

5. Discussion

First, the weighting ablation confirms that objective priority shapes the reported routing trade-off. Energy priority lowers AEC, reliability priority favors PDR, and overhead priority favors PoH. This finding follows from exact comparison of the source-level candidate sets and should be attributed to the objective formulation, not to a metaheuristic search advantage.

Second, at 200 nodes the energy-priority formulation lowers mean AEC by 23.35% relative to the ETX-minimizing/MRHOF-like path reference, while differences in the reported secondary endpoints remain small. The energy-greedy baseline confirms that further energy reduction is possible at the cost of higher overhead and delay. The evidence therefore supports an energy-centered compromise rather than universal performance dominance.

Third, the network-wide ablation isolates a search contribution: full NAmbOA reaches lower final fitness than both component-only variants over 30 paired instances. Convergence iteration does not differ significantly, so no faster-convergence claim is warranted. The result is specific to the stated coupled encoding and controlled budget.

Several limitations remain. The simulator is a controlled path-level model rather than a packet-level standards implementation; AEC is model-calibrated; synthetic links repair disconnected topologies; and node count and density vary together in the fixed area. The ETX-minimizing/MRHOF-like method is a path-selection analogue, not a complete implementation of MRHOF. CT and APL affect selection but are not included in the available outcome tables, and comparisons do not yet include other general-purpose optimizers under the same network-wide budget.

The present evidence should therefore be interpreted as controlled proof of concept. Full reproduction additionally requires the simulator implementation, configuration, random seeds, candidate sets, and run-level outputs. These materials should accompany a revised submission as supplementary files. External validation in Contiki-NG/Cooja or an equivalent environment, with heterogeneous traffic, interference, mobility, and hardware-aware energy measurement, remains necessary.

6. Conclusion

This study presents an energy-prioritized multi-objective routing framework for DODAG-constrained 6LoWPAN networks and a separate NAmbOA network-wide search study. At source level, the small candidate sets are evaluated exhaustively; NAmbOA is not claimed to be necessary for that task.

Energy-priority weighting reduces mean AEC relative to balanced weighting and to an ETX-minimizing/MRHOF-like path reference under the controlled simulator. These gains must be read together with the reported overhead, delay, and delivery trade-offs and the absence of CT and APL outcome summaries.

In the coupled network-wide ablation, full NAmbOA achieves lower final fitness than the NiOA-inspired and CAOA-inspired component-only variants, but no significant convergence-speed advantage is observed. This supports a bounded hybridization claim under the tested encoding and budget, not general algorithmic superiority.

Future work will evaluate NAmbOA in full RPL/6LoWPAN simulation environments such as Contiki-NG/Cooja and under more realistic conditions, including heterogeneous traffic, mobility, interference, and hardware-aware energy models. Adaptive objective weighting and larger DODAG-compatible search spaces will also be investigated.

Reproducibility statement

The equations and parameterization of the controlled simulator are specified above. A revised submission should include the implementation, configuration file, random seeds, candidate-route sets, and run-level outputs as supplementary material so that the numerical tables and statistical tests can be independently reproduced.

References

[1] T. Winter et al., “RPL: IPv6 Routing Protocol for Low-Power and Lossy Networks,” RFC 6550, Mar. 2012, doi: 10.17487/RFC6550.

[2] S. Mokrani, M. Belkadi, T. Sadoun, J. Lloret, and R. Aoudjit, “LEA-RPL: lightweight energy-aware RPL protocol for internet of things based on particle swarm optimization,” Telecommunication Systems, vol. 88, Art. no. 14, 2025, doi: 10.1007/s11235-024-01254-y.

[3] V. C. Diniesh, B. Palaniswamy, L. Murali, N. Manikandan, and K. Ramaswamy, “Improved energy efficient load balanced mobility management RPL protocol for mobile internet of things networks,” Scientific Reports, vol. 15, Art. no. 43199, 2025, doi: 10.1038/s41598-025-27253-w.

[4] M. Tarif, M. Homaei, A. Mirzaei, and B. Nouri-Moghaddam, “Optimizing RPL Routing Using Tabu Search to Improve Link Stability and Energy Consumption in IoT Networks,” Computers, Materials & Continua, vol. 87, no. 1, Art. no. 87, 2026, doi: 10.32604/cmc.2025.071676.

[5] M. R. Poornima, H. S. Vimala, and J. Shreyas, “Fuzzy-Based Novel Cross-Layer RPL Objective Function for Energy-Aware Routing in IoT,” International Journal of Computational Intelligence Systems, vol. 18, Art. no. 182, 2025, doi: 10.1007/s44196-025-00916-2.

[6] M. Lmkaiti, M. Lachgar, I. Larhlimi, H. Moudni, and H. Mouncif, “Secure Optimization of RPL Routing in IoT Networks: Analysis of Metaheuristic Algorithms in the Face of Attacks,” International Journal of Advanced Computer Science and Applications, vol. 16, no. 4, 2025, doi: 10.14569/IJACSA.2025.01604113.

[7] S. Remya, M. J. Pillai, C. Arjun, S. Ramasubbareddy, and Y. Cho, “Enhancing Security in LLNs Using a Hybrid Trust-Based Intrusion Detection System for RPL,” IEEE Access, vol. 12, pp. 58836–58850, 2024, doi: 10.1109/ACCESS.2024.3391918.

[8] V. R. Rajasekar and S. Rajkumar, “FPES-IDS: Forecast-Path and Exponential Smoothing-Based Intrusion Detection System to Mitigate Blackhole Attack in RPL-Based 6LoWPANs,” IEEE Access, vol. 13, pp. 67170–67195, 2025, doi: 10.1109/ACCESS.2025.3557670.

[9] A. Berguiga, A. Harchay, and A. Massaoudi, “HIDS-RPL: A Hybrid Deep Learning-Based Intrusion Detection System for RPL in Internet of Medical Things Network,” IEEE Access, vol. 13, pp. 38404–38429, 2025, doi: 10.1109/ACCESS.2025.3545918.

[10] E.-S. M. El-Kenawy et al., “NiOA: A Novel Metaheuristic Algorithm Modeled on the Stealth and Precision of Japanese Ninjas,” Journal of Artificial Intelligence in Engineering Practice, vol. 1, no. 2, pp. 17–35, 2024, doi: 10.21608/jaiep.2024.386693.

[11] X. Xu, “Crocodile Ambush Optimization Algorithm: A new bio-inspired metaheuristic algorithm for solving optimization problems,” Array, vol. 28, Art. no. 100529, 2025, doi: 10.1016/j.array.2025.100529.

[12] O. Gnawali and P. Levis, “The Minimum Rank with Hysteresis Objective Function,” RFC 6719, Sep. 2012, doi: 10.17487/RFC6719.